Proceedings of the TMCE 2010, April 12–16, 2010, Ancona, Italy, Edited by I. Horváth, F. Mandorli and Z. Rusák

THE CHINESE FACE: A 3D ANTHROPOMETRIC ANALYSIS

Yan Luximon
SizeChina lab, School of Design
The Hong Kong Polytechnic University
sdtina@polyu.edu.hk

Roger Ball
SizeChina lab, School of Design
The Hong Kong Polytechnic University
Sdroger@polyu.edu.hk

Lorraine Justice
School of Design
The Hong Kong Polytechnic University
lorraine.justice@polyu.edu.hk

Figure 1 The 3D head scans from SizeChina survey (Everyone's face is different)

ABSTRACT

Traditional facial anthropometry has a long history yet few studies have been conducted using the latest 3D scanning technology. The majority of these facial studies have focused on Caucasian populations. The recent SizeChina survey has collected high resolution 3D data from over 2000 adult Chinese subjects. The 3D facial data of 772 females from the SizeChina database were analyzed in this study. This data was pre-processed to eliminate scan noise, fill holes caused by shadow effect and aligned to a common plane. Thirty one facial landmarks were used for statistical analysis and to create a 3D anthropometric face model. Simple statistics results demonstrated that Chinese females in general have wider and shorter faces compared to other cultures. Correlation analysis showed the breadth dimensions are highly correlated and it seems that heavier people have larger bigonial breadth. Results from the principal component analysis on anthropometric face model reveals that major variations of face shapes are related to face breadth, face depth, face length, chin and jaw position. The results of this study have significant implications for the design of facial products for Chinese women.

KEYWORDS

China, face, 3D, anthropometry, design, ergonomics

1. INTRODUCTION

The human body varies by race, gender, age and many other factors. The human face, as an icon of identification, attracts the greatest scrutiny. Everyone's face is unique to them (Figure 1). Many attempts have been made to measure and categorize human faces. Traditional anthropometry uses a lot of numerical dimensions to describe the face shape [1]. Categories such as; oval, long-narrow, square, round, triangular are commonly used everywhere from the beauty business to medical studies. Traditional anthropometric measures are unsatisfactory for describing the complex geometry of the human face. An accurate detailed three dimensional model based on high resolution 3D scans is needed by industry to create better fitting and safer facial products. The

design and development of optical products such as protective safety goggles and surgical facemasks would benefit greatly from access to this type of highly detailed data. However very few studies have captured detailed 3D face shape data.

1.1. Anthropometry of human face

Anthropometric studies of human face have a long history however they are limited to linear dimensions such as face width and face length measured by calliper and tape directly on human face or through photography [1-6]. In addition, researchers have used traditional dimensions to provide product evaluation [7]. A recent survey of the head and face of Chinese workers [8-10] used 19 facial dimensions collected by traditional techniques to propose modifications to the design of a respirator.

Traditional measurements have been successfully used to design some facial products however drawbacks remain. Manual measurements are time consuming and require experience and physical contact between participants and researchers. The accuracy and repeatability vary widely depending on the researcher's expertise. There can be significant variations between individual researchers. Most importantly, traditional data is unable to describe the complex geometry of the head and face. Therefore, some researchers combined traditional measurements and 3D digital model to analyze the face shape and to test the fit of spectacle frames [11]. Further development of 3D digital models is important for product design.

1.2. 3D scanning and modelling

The recent development of 3D laser scanning technology has provided anthropometric researchers with the opportunity to overcome the limitations of traditional univariate data. Using 3D scanning, researchers are able to obtain 3D coordinates of human body shape. The Civilian American and European Surface Anthropometry Resource (CAESAR) project, one of earliest full body scan surveys, was completed using subjects from; USA, Netherlands and Italy [12]. Many recent studies utilized the data from CAESAR and other 3D human data bases [13-19]. Xi and Shu [16] used CAESAR data set to analyze the shape variation of the Caucasian head. However only a few high resolution 3D scanning surveys of the face have been achieved. Additionally there were only a few small scale and low resolution 3D scan surveys of the adult Chinese head and face [20, 21]. These surveys focused on young adult males of military service age which excluded females and other age groups.

1.3. The objective

The objective of this study is to analyze 3D faces of Chinese female adults using both traditional anthropometrical dimensions and 3D laser scanning technology. The results demonstrate the 3D face shape variation of Chinese women.

2. METHOD

2.1. Head and face data collection

The 3D anthropometric survey (SizeChina), was the first 3D head and face scan survey for the adult Chinese population [22]. The survey used a combination of traditional anthropometric methods (caliper and tape) and laser scanning technologies (Cyberware 3030 Color 3D scanner) to create a high resolution 3D digital database of Chinese head shapes. The survey followed international standards for the collection of statistically accurate 3D data. The six selected locations followed the sampling locations of a traditional anthropometric survey that was conducted in mainland China in 1988 [23]. The scan locations were distributed in north, south, east and central China. Equal amounts of male and female civilian subjects were scanned and there were no restrictions on the height, weight or social status of subjects.

Subjects' basic information including age, gender, family background, and the location where they grew up was collected using a written questionnaire. Traditional anthropometric measurements were recorded afterwards. Following ISO 7250, the head length and head width were taken using an anthropometer and the head circumference was measured using a tape. A trained expert was responsible to put fourteen landmarks on subject's face to identify the critical positions. Those fourteen landmarks were Chin, Glabella, Frontotemporale (left and right), Infraorbitale (left and right), Pronasale, Sellion, Tragion (left and right), Zygofrontale (left and right) and Lat. zygomatic (left

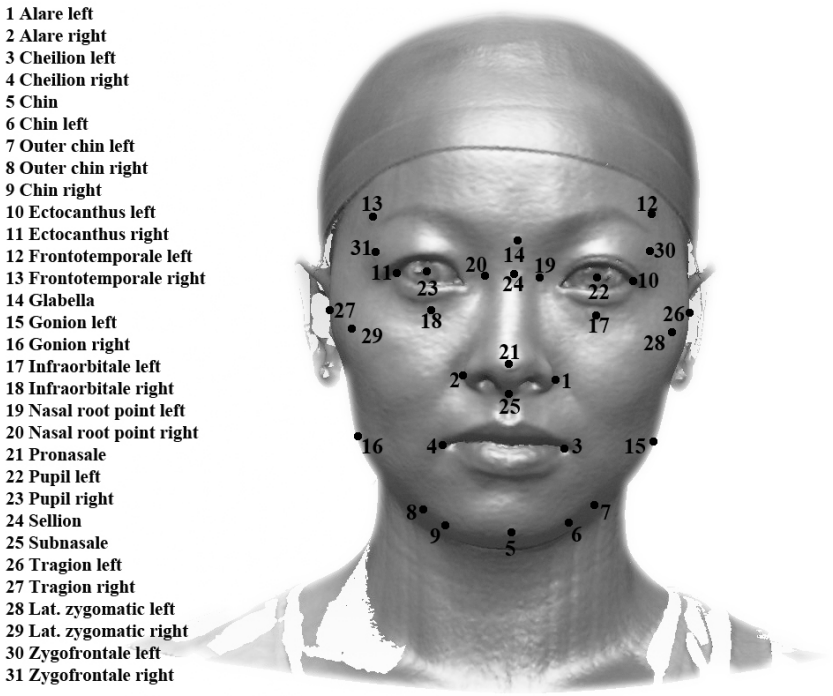

Figure 2 The head scan example with 31 landmarks

and right) (Figure 2). The anatomical definitions of all these landmarks are listed in Appendix 1. In order to minimize the error caused by hair, a tight fitting nylon wig cap was fitted to each subject's head. Subject sat on a chair located in the middle of the scanner and it took 17 seconds to finish one scan. The point cloud data was captured automatically through the Cyberware equipment.

2.2. Data process

2.2.1. Noise eliminating and holes filling

The original scan data has many "scan noise" which is extra data points or "holes" which is missing data (Figure 3 (a)). Extra data can be caused by clothing, accessories or lighting. Missing data normally occurs when the laser light can not cover the region such as top of the head, ear and nose. In this study, the noise and holes of original data were repaired in Rapidform software (www.rapidform.com) (Figure 3 (b)).

(a) Original scan (b) After cleaning noise and filling holes

Figure 3 Noise cleaning and holes filling for scan data

2.2.2. 3D head alignment

Even though the subjects were sitting in the center of the scanner, the head might rotate and shift from

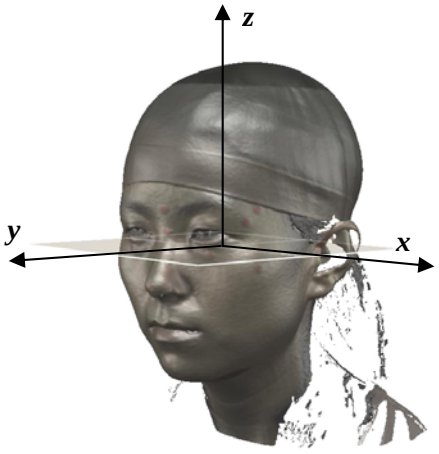

Figure 4 Alignment based on Frankfurt plane

subject to subject. In order to use consistent coordinates, all scan data was aligned in DigiSize software (www.cyberware.com) based on the three landmarks including left infraorbitale, left and right tragions. The plane created by these three landmarks is commonly called Frankfurt plane (Figure 4). The scan data were transferred into new coordinates after alignment.

2.2.3. Landmarks selection

The 3D coordinates of 14 physical landmarks on subject's face (Figure 2) were obtained in DigiSize software. Seventeen additional landmarks were taken directly from software at the same time (Alare (left and right), Cheilion (left and right), Chin (left and right), Outer chin (left and right), Ectocanthus (left and right), Gonion (left and right), Nasal root point (left and right), Pupil (left and right) and Subnasale) (Figure 2). The selection of the landmarks was mainly based on the study of anthropology and head-and-face survey [17, 24]. In total, 31 landmarks were collected (Appendix 1).

Table 1 The simple statistics of univariate measurements for female (N=772)

	Mean	Std Dev	Mini-mum	Maxi-mum
Age (years)	41.99	15.70	18.00	84.00
Body Height (cm)	155.60	5.79	137.10	175.00
Body Weight (kg)	55.73	9.01	31.70	97.60
Head circumference (mm)	545.74	14.08	503.00	597.00
Minimum frontal breadth (12-13) (mm)	119.34	7.65	95.00	142.00
Interpupillary breadth (22-23) (mm)	65.56	4.26	52.00	78.00
Bitragial breadth (26-27) (mm)	149.34	8.85	126.00	182.00
Bigonial breadth (15-16) (mm)	127.20	9.36	98.00	162.00
Sellion-Subnasale length (24-25) (mm)	48.75	3.75	39.00	60.00
Subnasale-Chin length (25-5) (mm)	57.70	4.65	38.00	72.00

2.3. Data analysis

The statistics of traditional head and facial measurements and 3D facial landmarks were both analyzed. Univariate facial dimensions were calculated based on the landmarks in DigiSize software. These measurements included minimum frontal breadth (landmark 12 to 13), Interpupillary breadth (landmarks 22 to 23), Bitragial breadth (landmarks 26 to 27), Bigonial breadth (landmarks 15 to 16) in x direction, Sellion-Subnasale length (landmarks 24 to 25) and Subnasale-Chin length (landmarks 25 to 5) in y direction.

A 3D anthropometric face model was created by making a triangle mesh based on the 3D landmark data of each subject. An average anthropometric face model was calculated by averaging x, y and z coordinates of each landmark.

Further analysis was completed using Principle Component Analysis (PCA) [25]. PCA uses linear combination of principal components (PC) to decompose the raw data using covariance matrix so that reducing the number of variables. The interested PC in principal component space can be translated back into the space of raw data and visually represent the results more clearly. The shape variables (3D coordinates) of aligned landmarks of head scan data were the input in PCA in this study. In total, the raw input variables were equal to 93 (31 landmarks×3 dimensions).

3. RESULTS

3.1. Simple statistics

The total number of scans for female Chinese was more than 1000 and 772 subjects were selected for this study due to the quality of scanning. The simple statistics of subjects' information and those univariate measurements are shown in Table 1.

3.2. The correlation analysis

The correlation coefficients among univariate measurements of Chinese female were calculated (Table 2).

Table 2 The correlation coefficients among univariate measurements for Chinese female (N=772)

	Age	Body height	Body weight	Head Circum-ference	Minimum frontal breath	Inter-pupillary breadth	Bitragial breadth	Bigonial breadth	Sellion-Subnasale length
Body height	-0.32*								
Body weight	0.29*	0.30*							
Head circumference	-0.01	0.30*	0.41*						
Minimum frontal breath	-0.11***	0.32*	0.35*	0.30*					
Interpupillary breadth	-0.20*	0.28*	0.15*	0.34*	0.37*				
Bitragial breadth	-0.08	0.31*	0.23*	0.34*	0.28*	**0.51***			
Bigonial breadth	0.12**	0.19*	**0.58***	0.41*	0.29*	0.42*	**0.62***		
Sellion-Subnasale length	0.28*	0.13**	0.15*	0.17*	0.11**	-0.07	-0.07	-0.07	
Subnasale-Chin length	0.29*	0.12**	0.36*	0.20*	0.17*	0.03	0.02	0.14*	0.15*

Note: *p <0.0001 **p<0.001 ***p<0.01

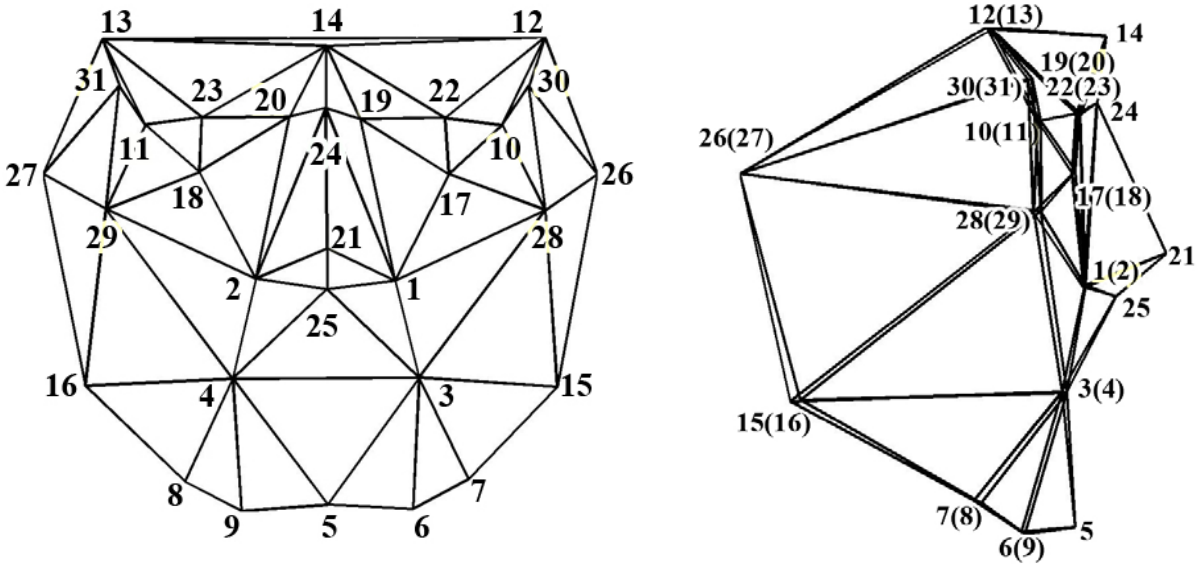

(a) The front view (b) The side view

Figure 5 The average anthropometric face model of Chinese female

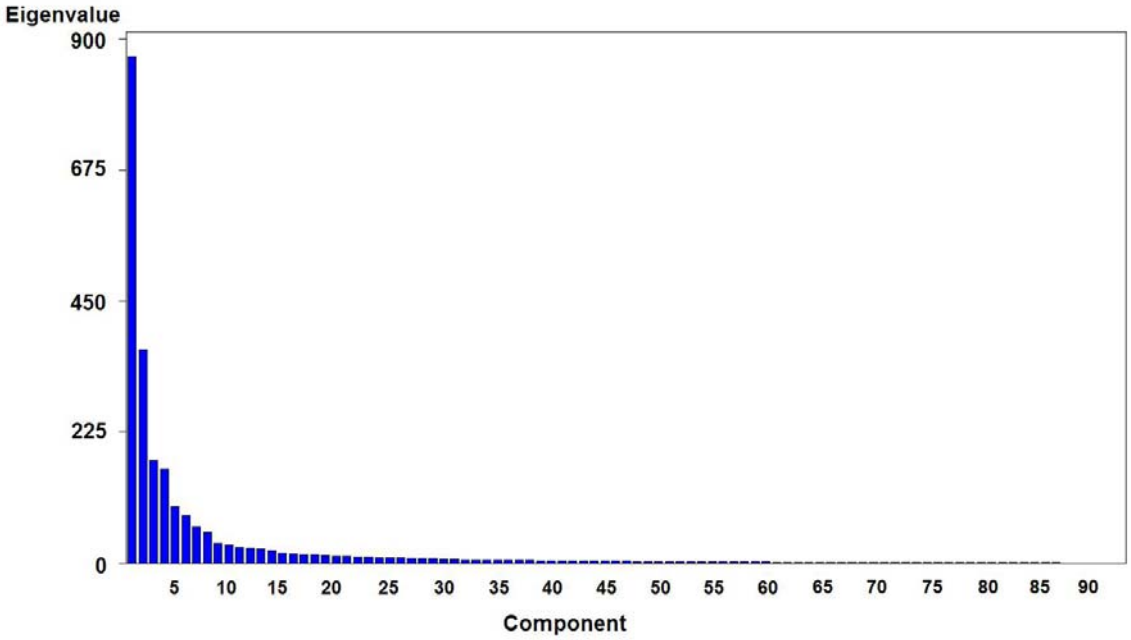

Figure 6 The Eigenvalue of principle component analysis

Results showed that body weight was highly related to bigonial breadth (correlation coefficient = 0.58, $p<0.0001$). That is to say, subject's bigonial breadth tends to be larger if the subject is heavier. In addition, interpupillary breadth and bitragial breadth (correlation coefficient = 0.51, $p<0.0001$), bitragial breadth and bigonial breadth (correlation coefficient = 0.62, $p<0.0001$) had significantly positive correlations. These results showed that people who have wider face, have larger eye distance and more lateral jaw structure in general.

3.3. Average anthropometric face model

Based on the average 3D coordinates of all 31 landmarks, an average anthropometric face model of Chinese female was created (Figure 5) by averaging the coordinates of the landmarks for all the participants. The anthropometric face model is symmetrical and appears oval in shape.

3.4. Principle component analysis (PCA)

Principle component analysis was performed for 772 Chinese female data. The 93 shape variables from 31 landmarks were the input variables for PCA. The result of eigenvalue calculation from covariance matrix is presented in Figure 6.

A series of principal components (PCs) was created in PC space. All the subsequent PC was orthogonal to preceding PC. The first principal component (PC1) contained the highest amount of variation (37.58%); the second principal component (PC2) represented the second highest amount of variation (15.86%), and so forth. From the ninth PC, the eigenvalue did not have obvious difference from the next one. Therefore, the first eight PCs were discussed more in detail to view the variations of face shape. The

Table 3 The eigenvalue of principle components using covariance

Principle component	Eigenvalue	Cumulative percentage
1	869.20	37.58%
2	366.76	53.44%
3	175.82	61.04%
4	161.07	68.01%
5	96.45	72.18%
6	80.98	75.68%
7	62.99	78.4%
8	52.36	80.67%

eigenvalue and cumulative percentage of total variance of the first 8 PCs are presented in Table 3. They contained 80.67% of the total variance.

In order to visually represent the first eight PC more clearly, the PCA algorithm was applied [25]. The PC variables were translated back into the space variables (3D coordinates) of raw data in xyz space through Equation (1).

$$D = \overline{D} + V \times P \quad (1)$$

where $\overline{D}$ is the average 3D coordinates of raw data; V is the inverse matrix of eigen-vector loading matrix; P is a column vector that decide the value for each principal component; D is the newly created set of shape variables in xyz space based on the value of the principal component. When setting P to be zero, D is equal to the average 3D coordinates. If the value of first cell of P is changing and all the other cells is kept zero, the change of D will demonstrate the variation along the first principal component representing the largest variance in the database.

By changing the value of first 8 cells of P one by one from negative three standard deviations to positive three standard deviations calculated from corresponding first 8 PCs, the variations along first 8 principal components are demonstrated in Figure 7. The variation of PC1 (Figure 7(a)) demonstrates that persons who have smaller faces (face breadth in x axis and face depth in y axis) and persons who have bigger faces would give a greatest variation for the face shape. The side view of PC1 shows that the positions of chin and jaw are also related to PC1. When the face is smaller, chin and jaw are more inside.

The second component (PC2) is related to the size of face in y and z axis (Figure 7(b)). The face changes from shorter to longer. Similar as PC1, chin and jaw are also related to PC2. However, when the face is shorter, chin and jaw are more outside.

The third and fourth components (PC3 and PC4) represent unsymmetrical faces (Figure 7(c) and Figure 7(d)). The face along PC3 tends to be right side is smaller than left side but the face along PC4 tends to be left side is smaller than right side.

The fifth component (PC5) relates to the upper face and jaw (Figure 7(e)). Person who has wider forehead tends to have larger jaw. The sixth component (PC6) is more related to chin and jaw (Figure 7(f)). Variation shows that person who has inside chin and small jaw is obviously different from the one who has outside chin and big jaw. In another word, PC6 represents the distance between chin and jaw.

The seventh and eighth components (PC7 and PC8) clearly relate to the breath of face (Figure 7(g) and Figure 7(h)). The face shape varies along PC7 with different wideness but same face length. At the same time, chin and jaw have slightly changes. Similarly, the face breadth varies along PC8 but with same face length. At the same time, nose and chin have some changes in the y direction.

4. DISCUSSION

Facial anthropometric dimensions have been studied for many years in different countries. In this study, six numerical measures of Chinese females were calculated. Comparing the results of previous studies in the literature, obvious racial differences can be observed. In general, Chinese females have bigger jaw, wider interpupillary distance, shorter chin than Koreans, French and Americans. The bigonial breadth was 127.20mm (mean) in this study, wider than French (97.1mm) [5], Koreans (106.1mm) [7], Americans (110.1mm) [18] and North American Caucasians (94.5mm) [1]. This breadth is comparable with Yang and Shen's study on Chinese (125.1mm) [10] but larger than Du et al.'s result (114.2mm) on Chinese workers [9]. In terms of interpupillary breadth, result from this study was 65.56mm, which is larger than Americans (61.9mm) [18] and previous studies on Chinese (61.0mm [9] and 61.04mm [6]). Obviously, subnasale-chin length of Chinese female (57.7mm) is shorter than African Americans (67.0mm) [4] and North American Caucasians (64.3mm) [1]. In a word, Chinese female faces are wider and shorter compared to French, Americans and Koreans.

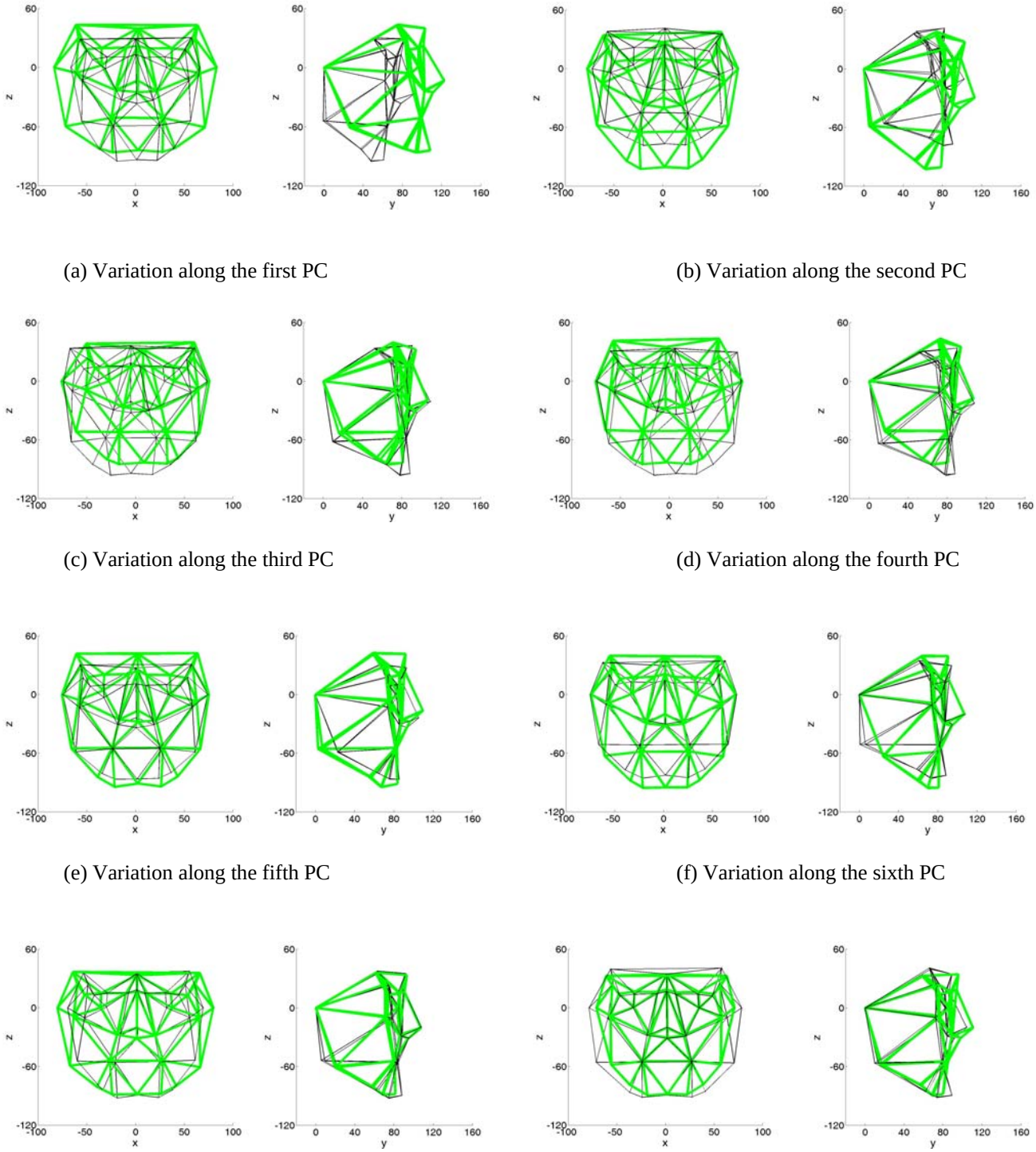

(a) Variation along the first PC

(b) Variation along the second PC

(c) Variation along the third PC

(d) Variation along the fourth PC

(e) Variation along the fifth PC

(f) Variation along the sixth PC

(g) Variation along the seventh PC

(h) Variation along the eighth PC

Figure 7 The face shape variations along first eight principle components

Correlation analysis showed that body weight was highly correlated to bigonial breadth in lower face but not upper and middle face breadth. This is expected due to the face anatomical structure. Moreover, bitragial breadth was highly positively correlated to bigonial breadth and interpupillary breadth. That is to say, the dimensions for measuring breadths are somehow highly related. These are consistent with the other anthropometric studies [7, 9].

The numerical measures from this study were slightly different from some of traditional measures on Chinese [9]. One of the reasons might be the differences between scan data method and traditional method. Traditional method is manually performed and physical contact of skin may cause the error of the dimensions. Bradmiller and Friess [17] also discussed the differences and suggested that traditional method might have more errors.

The analysis on 3D landmarks demonstrated very interesting results. More than 80% variance could be explained by first eight components. The visual representation of face variations along the components showed that face shape did not vary proportionally. The changes in face breadth and face depth were the biggest variation in all components. This was different from the result on Americans [17]. In their study, face breadth, face length and chin position gave largest variation in first principal component. Unlike Bradmiller and Friess's study [17], the result of our study included absolute size as important component in understanding facial anthropometrics. Therefore, our result presented all the variances within the samples and provides a recommendation to consider when creating a sizing system for designing facial products. It is suggested that not only face breadth but also face depth are important dimensions for designing eyewear and face masks.

5. CONCLUSION

In this study, facial dimensions were calculated and a 3D anthropometric face model was created based on facial landmarks of 772 Chinese adult females. Compared with Americans and other Asians such as Koreans, the Chinese female's faces were wider and shorter. The 3D shape analysis on facial landmarks demonstrated the first eight components representing more than 80% variance. The shape of human face did not vary proportionally. The changes in face breadth and face depth were the biggest variation. Other large variations included face length, chin and jaw. Results of the study give a basic picture of the different face shapes of Chinese females. This study has provided an example of how 3D scan data can be processed into a practical model for the design of facial products such as spectacles, surgical mask and respirators.

ACKNOWLEDGMENTS

The author would like to thank the Hong Kong Polytechnic University for supporting this work through Postdoctoral fellowship scheme (G-YX2Y).

APPENDICES

The landmarks' names and definitions are listed in Appendix 1.

REFERENCES

[1] Farkas, L. G., (1994), Anthropometry of the Head and Face. Raven Press, New York, NY, USA.

[2] Choe, K. S., Sclafani, A. P., Litner, J. A., Yu, G. P., and Romo, T. 3rd., (2004), "The Korean American Woman's Face: Anthropometric Measurements and Quantitative Analysis of Facial Aesthetics", Archives of facial plastic surgery, 6 (4), pp. 244-252.

[3] Le, T. T., Farkas, L. G., Ngim, R. C. K., Levin, L. S., and Forrest, C. R., (2002), "Proportionality in Asian and North American Caucasian Faces Using Neoclassical Facial Canons as Criteria", Aesthetic Plastic Surgery, 26(1), pp. 64-69.

[4] Porter, J. P., (2004), "The Average African American Male Face: An Anthropometric Analysis", Archives of facial plastic surgery, 6 (2), pp. 78-81.

[5] Coblentz, A., Mollard, R., Ignazi, G., (1991), "Three-dimensional face shape analysis of French adults, and its application to the design of protective equipment", Ergonomics, 34 (4), pp. 497-517.

[6] Quant, J. R., and Woo, G. C., (1992), "Eye position and head size in the Chinese population: A comparison of the Chinese from Hong Kong with the Chinese from Guangdong province", Optometry and vision science, 69(10), pp. 793-796.

[7] Kim, H., Han, D. H., Roh, Y. M., Kim, K., and Park, Y. G., (2003), "Facial Anthropometric Dimensions of

Koreans and Their Associations with Fit of Quarter-Mask Respirators", Industrial Health, 41 (1), pp. 8-18.

[8] Chen, W., Zhuang, Z., Benson, S., Du, L., Yu, D., Landsittel, D., Wang, L., Viscusi, D., and Shaffer, R. E., (2009), "New Respirator Fit Test Panels Representing the Current Chinese Civilian Workers", Annals of Occupational Hygiene, 53(3), pp. 297-305.

[9] Du, L., Zhuang, Z., Guan, H., Xing, J., Tang, X., Wang, L., Wang, Z., Wang, H., Liu, Y., Su, W., Benson, S., Gallagher, S., Viscusi, D., and Chen, W., (2008), "Head-and-Face Anthropometric Survey of Chinese Workers", Annals of Occupational Hygiene, 52(8), pp. 773-782.

[10] Yang, L., and Shen, H., (2008), "A pilot study on facial anthropometric dimensions of the Chinese population for half-mask respirator design and sizing", International Journal of Industrial Ergonomics, 38, pp. 921-926.

[11] Kouchi, M., and Mochimaru, M., (2004), "Analysis of 3D face forms for proper sizing and CAD of spectacle frames", Ergonomics, 47(14), pp. 1499-1516.

[12] Robinette, K., Daanen, H., and Paquet, E., (1999), "The CAESAR project: A 3-D surface anthropometry survey", Proceedings of 2nd International Conference on 3D Digital Imaging and Modeling (3DIM'99), pp. 380-386.

[13] Allen, B., Curless, B., and Popovic, Z., (2003), "The space of human body shapes: reconstruction and parameterization from range scans", ACM SIGGRAPH 2003, San Diego, CA, USA.

[14] Azouz, Z. B., Rioux, M., Shu, C., and Lepage, R., (2006), "Characterizing human shape variation using 3D anthropometric data", The visual computer, 22 (5), pp. 302-314.

[15] ter Haar, F. B., and Veltkamp, R. C., (2008), "A 3D Face Matching Framework", Proceedings of Shape Modeling International (SMI 2008), pp. 103–110.

[16] Xi, P., and Shu, C., (2009), "Consistent parameterization and statistical analysis of human head scans", The visual computer, 25(9), pp. 863-871.

[17] Bradtmiller, B., and Friess, M., (2004), "A head-and-face anthropometric survey of U.S. respirator users", Anthrotech technical report for NIOSH/NPPTL.

[18] Zhuang, Z., and Bradtmiller, B., (2005), "Head-and-Face Anthropometric Survey of U.S. Respirator Users", Journal of Occupational and Environmental Hygiene, 2(11), pp. 567-576.

[19] Zhuang, Z., Bradtmiller, B., and Shaffer, R., (2007), "New respirator fit test panels representing the current U.S. civilian work force", Journal of Occupational and Environmental Hygiene, 4(9), pp. 647–59.

[20] Chen, X., Shi, M., Zhou, H., Wang, X., Zhou, G., (2002), "The 'Standard Head' for Sizing Military Helmet Based on Computerized Tomography and The Headform Sizing Algorithm", Acta Armamentarii, 23(4), pp. 476-480 (in Chinese).

[21] Wang, X., Zheng, W., Liu, B., Wang, R., Xiao, H., Ma, X., (2005), "Study on 3-dimentional digital measurement of face form in fighter pilots", Chinese Journal of Aerospace Medicine, 16(4), pp. 258-261 (in Chinese).

[22] Ball, R. M., and Molenbroek, J. F. M., (2008), "Measuring Chinese Heads and Faces", Proceedings of the 9th International Congress of Physiological Anthropology, Human diversity: Design for life. Delft, the Netherlands, pp. 150-155.

[23] Standards Administration of the Peoples Republic of China, GB10000-88, (1993), Human Dimensions of Chinese Adults (in Chinese). Standard Press of China: Beijing.

[24] Aulsebrook, W. A., Becker, P. J., and Iscan, M. Y., (1996), "Facial soft tissue thickness in the adult male Zulu", Forensic Science International, 79, pp. 83-102.

[25] Smith, L. I., (2002), A tutorial on principal components analysis. Maintained by Cornell University.

Appendix 1 The landmark list

Name	Number (in Figure 2)	Definition [17,24]
Alare left, right	1, 2	The lateral point on the flare or wing of the nose
Cheilion left, right	3, 4	The lateral point of the juncture of the fleshy tissue of the lips with the facial skin at the corner of the mouth
Chin	5	The most protruding point on the bottom edge of the chin, along the jawline
Chin left, right	6, 9	A point on the bottom edge of the chin, along the jawline, directly below the corner of the mouth landmark (cheilion)
Outer chin left, right	7, 8	A point on the bottom edge of the chin, along the jawline, below a point 1 cm to the side of the corner of the mouth landmark (cheilion)
Ecotocanthus left, right	10, 11	The outside corner of the eye formed by the meeting of the upper and lower eyelids
Frontotemporale left, right	12, 13	The point of deepest indentation of the temporal crest of the frontal bone above the browridges
Glabella	14	The forward-most (anterior) point on the frontal bone midway between the bony browridges
Gonion left, right	15, 16	The side-most (lateral) point on the back (posterior) angle of the jawbone (mandible).
Infraorbitale left, right	17, 18	The lowest point on the forward-facing (anterior) border of the bony eye socket
Nasal Root Point left, right	19, 20	The point on the side of the nasal root at a depth equal to one-half the distance from the top of the nose to the eyes
Pronasale	21	The point of the most forward-facing (anterior) projection of the tip of the nose
Pupil left, right	22, 23	A point in the center of the eye
Sellion	24	The point of the deepest depression of the nasal bones at the top of the nose where the nose meets the forehead
Subnasale	25	The point of intersection of the groove of the upper lip (philtrum) with the bottom (inferior) surface of the nose on the head's midline (midsagittal plane)
Tragion left, right	26, 27	The highest (superior) point on the juncture of the cartilaginous flap (tragus) of the ear with the head
Lat. zygomatic left, right	28, 29	The point on the most lateral curvature of the zygomatic bone
Zygofrontale left, right	30, 31	The side-most (lateral) point of the frontal bone as it surrounds the eye socket